Accepted Manuscript

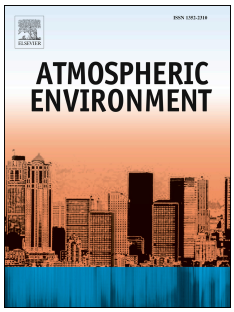

A budget analysis of the formation of haze in Beijing

Xuexi Tie, Qiang Zhang, Hui He, Junji Cao, Suqing Han, Yang Gao, Xia Li, Jiaxing Chan

PII: S1352-2310(14)00827-9

DOI: 10.1016/j.atmosenv.2014.10.038

Reference: AEA 13354

To appear in: *Atmospheric Environment*

Received Date: 31 July 2014

Revised Date: 17 October 2014

Accepted Date: 20 October 2014

Please cite this article as: Tie, X., Zhang, Q., He, H., Cao, J., Han, S., Gao, Y., Li, X., Chan, J., A budget analysis of the formation of haze in Beijing, *Atmospheric Environment* (2014), doi: 10.1016/j.atmosenv.2014.10.038.

Highlights

(1) A haze episode with a very strong variability in Beijing was analyzed.

(2) WRF-Chem and a box model are used for the budget analysis of haze formation.

(3) Under calm winds, a heavy haze can be formed in one (1) day.

(4) The wind speed to balance emission-clean processes was calculated.

A budget analysis of the formation of haze in Beijing

Xuexi Tie[1,2*], Qiang Zhang[3*], Hui He[3], Junji Cao[1], Suqing Han[4,] Yang Gao[3], Xia Li[3], Jiaxing. Chan[3]

[1]Key Laboratory of Aerosol Science and Technology, SKLLQG, Institute of Earth Environment, Chinese Academy of Sciences, Xi'an, China
[2]National Center for Atmospheric Research, Boulder, CO USA
[3]Beijing Weather Modification Office, Beijing, China
[4]Tianjin Weather Modification Office, Tianjin, China.

Corresponding Authors

(1) Xuexi Tie
xxtie@ucar.edu

(2) Qiang Zhang
zqxxm_cn@sina.com

Abstract

During recent winters, hazes often occurred in Beijing, causing major environmental problems. To understand the causes of this "Beijing Haze", a haze episode (from Oct. 21 to Oct. 31, 2013) in Beijing was analyzed. During the episode, the daily mean concentration of fine particulate matter ($PM_{2.5}$) reached a peak value of 270 μg/m^3 on Oct. 28, 2013, and rapidly decreased to 50 μg/m^3 the next day (Oct. 29, 2013). This strong variability provided a good opportunity to study the causes of a "Beijing Haze". Two numerical models were applied for this study. The first model is a chemical/dynamical regional model (WRF-Chem). This model is mainly used to study the effects that weather conditions have on $PM_{2.5}$ concentrations in the Beijing region. The results show that the presence of high air pressure in northwest Beijing (NW-High) generally produced strong northwest winds with clean upwind air. As a result, the NW-High played an important role in cleaning Beijing's PM. However, the NW-High's cleaning effect did not occur in every situation. When there was low air pressure in southeast Beijing (SE-Low) accompanied by a NW-High, an air convergent zone appeared in Beijing. The pollutants became sandwiched, producing high $PM_{2.5}$ concentrations in the Beijing region. The second model used in this study is a box model, which is applied to estimate some crucial parameters associated with the budget of $PM_{2.5}$ in the Beijing region. Under calm winds, the calculations show that continuous local emissions rapidly accumulate pollutants. The $PM_{2.5}$ concentrations reached 150 μg/m^3 and 250 μg/m^3 within one (1) day and two (2) days, respectively. Without horizontal dilution, this estimate can be considered as an upper time limit (the fastest time) for the occurrences of haze events in the Beijing region. The wind speed (WS_b) is calculated for the balance between the continuous emissions and atmospheric clean processes. The results show that the WS_b is strongly dependent on the planetary boundary layer (PBL) height and the wind direction. Under SE-Low weather conditions, the WS_b is 2 m/s with a higher PBL height (700 m). However, under lower PBL heights, the WS_b rapidly increases, reaching 4.5 m/s and 7.0 m/s with PBL heights of 300 m and 200 m, respectively. In contrast, under NW-High weather conditions, the WS_b reduces to 2.5 m/s and 4.0 m/s. These results suggest that when the prevailing wind in Beijing is a northwest wind (with wind speeds of > 4 m/s), particulate matter (PM) begins to decrease.

Keywords: $PM_{2.5,}$ Beijing, WRF-Chem, weather conditions

(1) Introduction

Beijing, the capital of China, is a mega city with a population of more than 20 million. In recent years, the city has experienced rapid economical development and growth. For example, in 2011, the number of automobiles was 5 million, and by 2016, this number is expected to be 6 million. In 2013, the increase of gross domestic product (GDP) was 7.7%. One negative byproduct of this rapid economical development, especially in the past two decades, is that Beijing has been forced to endure heavy air pollution, with particulate matter (PM) being one of its top pollutants (Chan and Yao, 2008). The high concentration of PM causes a wide range of environmental consequences. According to a study by Tie et al. (2009), exposure to extremely high particle concentrations leads to a great increase of lung cancer cases. High PM concentrations also significantly reduce the range of visibility (Deng et al., 2008; Cao et al., 2012) and enhance atmospheric acidity (Cao et al., 2013) in China's large cities. However, high PM concentrations also have a bright side – they reduce the photochemical production of ozone, which is another harmful pollutant affecting human health (Tie et al., 2005; Bian et al., 2007; Tie and Cao, 2009).

In the last decade, extensive efforts have been made to characterize the sources, properties, and processes of PM in Beijing. Recent studies indicate that a large mass fraction of ambient PM in Beijing is fine particles, of which carbonaceous particles, sulfate, nitrate, and ammonium are major components (Guinot et al., 2007; He et al., 2001; Yang et al., 2011). The different sources that contributed to Beijing's PM concentrations have also been studied (Zhang et al., 2013). Despite progress made by previous studies, there are still some important questions to be answered and addressed. In recent years, high concentrations of particle concentrations are occurring frequently in Beijing and its surrounding regions (Zhang et al., 2006; 2009), and a very large variability of PM concentrations is often characterized (He et al., 2014). It is interesting to note that PM concentrations increase exponentially in the span of a few days, with non-linear growth. According to a study by Quan et al. (2013), this rapid increase in PM concentrations might involve an interaction between particles and the planetary boundary layer (PBL); however, more studies are still needed in this area.

In order to analyze the causes and variability of PM in Beijing, a high aerosol pollution episode, characterized by a large variability of PM concentration is studied. The episode occurred between Oct. 21 and Oct. 31, 2013. During the episode, the daily mean concentration of $PM_{2.5}$ reached a peak value of 250 $\mu g/m^3$ on Oct. 28, 2013, and rapidly decreased to 50 $\mu g/m^3$ the next day (Oct. 29, 2013). This strong variability provided a good opportunity to study the causes of a "Beijing Haze". Two numerical models are applied in this study. The first model is a chemical/dynamical regional model (WRF-Chem). The WRF-Chem model is a state of the art regional dynamical/chemical/aerosol model. This model is mainly applied to study the effects of weather conditions on the regional transport and distribution of PM. The second model is a box model, and this model is mainly used for the budget analysis of the mass of PM in Beijing, such as quantifying the effect of surface emission accumulation on the growth of PM and the advection of PM with different meteorological parameters (wind direction, wind speed, and the PBL height) in the Beijing region.

(2) Methods

Numerical models are extensively used in this study. The first model is a state of the art regional dynamical/chemical/particle model (WRF-Chem), and the second model is a box model. Detailed descriptions of the models are as follows:

2.1 WRF-Chem Model

The main objectives of this study are to apply a regional chemical/dynamical model, to analyze measurements, to evaluate the model by comparing the model result to the measured data, and to study $PM_{2.5}$ variability in the Beijing region. The model used in this study is a regional chemical/transport model (Weather Research and Forecasting Chemical model – WRF-Chem). There are two major parts of the model, namely, a dynamical model (WRF) and a chemical model (Chem). The Weather Research and Forecasting (WRF) Model is a next-generation mesoscale numerical weather prediction system designed to serve both operational forecasting and atmospheric research needs. The effort to develop WRF has been a collaborative partnership, principally

among the National Center for Atmospheric Research (NCAR), the National Centers for Environmental Prediction (NCEP), the Forecast Systems Laboratory (FSL), the National Oceanic and Atmospheric Administration, the Air Force Weather Agency (AFWA), the Naval Research Laboratory, Oklahoma University, and the Federal Aviation Administration (FAA). The WRF model is a fully compressible and non-hydrostatic Euler model. Thirty-five vertical levels are used in a stretched vertical grid with spacing ranging from 50 m near the surface, to 500 m at 2.5 km and 1 km above 14 km. The model employs the Lin microphysics scheme (Lin et al., 1983), the Yonsei University (YSU) PBL scheme (Noh et al., 2001), the Noah land-surface model (Chen and Dudhia, 2001), the long-wave radiation parameterization (Mlawer et al., 1997), and the shortwave radiation parameterization (Dudhia, 1989). Detailed information regarding the parameters used in the WRF model, such as the PBL scheme, the land surface scheme, the microphysics scheme, and the cumulus cloud scheme can be found at the WRF website (http://www.wrf-model.org/wrfadmin/docs/arw_v2.pdf), and the WRF model is documented by Skamarock et al. (2008).

In addition to dynamical calculations, a chemical model is "online" coupled with the WRF model (WRF-Chem). Grell et al. (2005) provides more details about the WRF-Chem. The version of the model used in the present study (Tie et al. 2007) includes an online calculation of dynamical inputs (winds, temperature, boundary layer, clouds, etc.); transport (advection, convection, and diffusion); dry deposition (Wesely, 1989); gas phase chemistry, radiation, and photolysis rates (Madronich and Flocke, 1999; Tie et al., 2003), and surface emissions (including an online calculation of biogenic emissions). The chemical mechanism used is the RADM2 (Regional Acid Deposition Model, version 2) gas-phase chemical mechanism (Chang et al., 1989), which includes 158 reactions among 36 species. The aerosol modules used in the study are described as the aerosol module developed by EPA CMAQ (version 4.6) (Binkowski and Roselle, 2003). The inorganic aerosols are predicted in the WRF-Chem model using ISORROPIA (version 1.7) (http://nenes. eas.gatech.edu/ISORROPIA/), which calculates the composition and phase state of an ammonium-sulfate-nitrate-chloride-sodium-calcium-potassium-magnesium-water inorganic aerosol in thermodynamic equilibrium with gas phase precursors. The secondary organic aerosol (SOA) formation is simulated using a non-traditional SOA model including the volatility basis-set modeling method in which primary organic components are assumed to be semi-

volatile and photo-chemically reactive and are distributed in logarithmically-spaced volatility bins as previously described (Li et al., 2011).

In this study, the domain of the numerical simulation is 1000×1000 km in a horizontal region that is centered in Beijing City with a resolution of 10 km. The chemical lateral boundary conditions are constrained from the result of a global chemical transport model (MOZART–Model for OZone And and Related chemical Tracers), with the aerosol formation modules (Tie et al., 2005; Emmons et al., 2010). The model ran from Oct. 16 to Oct. 31, 2013, and only the results from the last 10 days (from Oct. 21 to Oct. 31) were used (the results from the first five (5) days are considered as spin up of the model calculations). The hourly emissions in the region are based on the data-base constructed by Streets et al. (2003; 2008), with a horizontal resolution of 0.16˚. The emissions are interpreted into the model resolution (10 km). The emission is evaluated and adjusted (due to the changes in different years between the inventory and model calculation) by the study of He et al. (2014).

2.2 Box Model

In order to perform a budget analysis, a simple box model, which is suitable for Beijing City is established in this study. According to mass conservation, the $PM_{2.5}$ concentration [X] can be calculated by the following equation:

$$\partial[X]/\partial t = \partial[X]/\partial t]_E + \partial[X]/\partial t]_T + \partial[X]/\partial t]_V + \partial[X]/\partial t]_C + \partial[X]/\partial t]_D \quad (1)$$

Where $\partial[X]/\partial t$ represents the local change rate of $PM_{2.5}$ concentrations in Beijing; $\partial[X]/\partial t]_E$ represents the change rate due to surface emissions; $\partial[X]/\partial t]_T$ is the change rate due to advection; $\partial[X]/\partial t]_V$ is the change rate due to vertical mixing; $\partial[X]/\partial t]_C$ is the change rate due to chemical reactions; and $\partial[X]/\partial t]_D$ is the change rate due to surface deposition.

For the budget analysis, several assumptions were made in this study, including (1) for $\partial[X]/\partial t]_C$, the main chemical reactions correspond to the particle chemical formation (secondary particles). In this case, we added this term into the emission term

$(\partial[X]/\partial t]_{EC} = \partial[X]/\partial t]_E + \partial[X]/\partial t]_C)$; (2) the particles are well mixed and uniformly distributed inside the PBL height; (3) in a short period, the deposition term $(\partial[X]/\partial t]_D)$ is small, especially for fine particles; and (4) in order to perform the budget analysis in Beijing City, we defined a horizontal box as Beijing City, with the city length and width of 100 km (shown in Fig. 1).

Under the above assumptions and definitions, Eq. (1) is simplified to Eq. (2)

$$\partial[X]/\partial t = \partial[X]/\partial t]_{EC} + \partial[X]/\partial t]_T + \partial[X]/\partial t]_V \qquad (2)$$

Where $\partial[X]/\partial t]_{EC}$ represents the change rate due to both surface emissions and secondary aerosol formation. With the assumption that the particles are well mixed inside the PBL, and the transport between the PBLH and the free troposphere is neglected, the mean concentration in the box can be calculated by

$$[X]_{t+1} = [X]_t + \frac{EM}{PBLH} \times \Delta t + \{(WS \times [X])_{in} - (WS \times [X])_{out}\}/DL \times \Delta t \qquad (3)$$

Where $[X]_{t+1}$ and $[X]_t$ represents the $PM_{2.5}$ concentration at time t and t+1 ($\mu g/m^3$), and EM represents surface emissions ($\mu g/s/m^2$). PBLH stands for the PBL height (m); Δt is the time step (1 hour); WS is the wind speeds at 10 m (m/s); $[X])_{in}$ is the $PM_{2.5}$ concentration at the upwind boundary; $[X])_{out}$ is the $PM_{2.5}$ concentration at the downwind boundary; and DL is the city length (m). In later sections, we demonstrated some important information regarding the formation of hazes, which can be obtained by a simple box model.

(3) Results and discussion

3.1 Variability of $PM_{2.5}$ concentrations

The calculated $PM_{2.5}$ concentrations were compared with the measured $PM_{2.5}$ concentrations in Beijing. The measurement was provided by routine measurements from the

Chinese Environment Protection Administration (Chinese EPA). Based on the availability of data, this study used five (5) sites. Among the five (5) sites, two (2) are located in the center of the city (Dongshi (116.4239E, 39.9305N) and Auti (116.4068E, 39.9909N), and three (3) are at the edge of the city (Shunyi (116.6616E, 40.1367N), Huairuo (116.6378E, 40.3226), and Changping (116.2366E, 40.2264N)). The measured $PM_{2.5}$ concentrations are hourly values, and the daily averaged values were computed for the study.

Surface emissions of $PM_{2.5}$ (g/s) were noted for each model grid (see Fig. 2). As the northwest area of Beijing has mountains and grasslands, with a very small population, the northwest wind transports clean air to Beijing (as shown by the white arrow). In contrast, in the south of Beijing, the population is very dense, with several mega/large cities. Thus, high $PM_{2.5}$ emissions are located in the south of Beijing, and the south wind transports polluted air to Beijing (as shown by the black arrow).

The measured data was averaged to represent mean concentrations in Beijing (as shown in the red bars in Fig. 3). $PM_{2.5}$ concentrations in a pollution episode from Oct. 21 to Oct. 31, 2013 in Beijing were calculated and measured. This episode was chosen because it has unique properties for analyzing the causes of heavy hazes in Beijing. First, during this period, $PM_{2.5}$ concentrations were high, with the maximum daily averaged concentrations of 270 $\mu g/m^3$. According to the definition by the Chinese Meteorological Administration (CMA), a haze event is defined by the following conditions: visibility < 10 km and RH < 90%. According to the studies by Deng et al. (2008) and Cao et al. (2012), the $PM_{2.5}$ concentrations corresponding to the definition of CMA ranged from a daily mean of 50-100 $\mu g/m^3$. Thus, the $PM_{2.5}$ concentrations can be considered as a heavy haze event. Second, there was a strong variability of the $PM_{2.5}$ concentrations. For example, there were three (3) maxima and two (2) minimums during the episodes. In order to understand the causes of the strong variability better, four periods (P-1, P-2, P-3, and P-4) were defined in the analysis. During P-1 (from Oct. 21 to Oct. 23, 2013), the $PM_{2.5}$ concentrations were high on Oct. 21 and 22 (with daily averaged concentrations of 75-120 $\mu g/m^3$), and decreased to a low value on Oct. 24 (20 $\mu g/m^3$). During P-2 (from Oct. 23 to Oct. 28), the $PM_{2.5}$ concentrations were low from Oct. 24 to Oct. 26 (less than 50 $\mu g/m^3$), and then rapidly increased to very high values on Oct. 27 and 28 (with daily averaged concentrations of 170-270

μg/m^3). During P-3 (from Oct. 28 to Oct. 29), the $PM_{2.5}$ concentrations rapidly decreased from a very high value (270 μg/m^3) to a low value (50 μg/m^3). During P-4 (from Oct. 29 to Oct. 31), the $PM_{2.5}$ concentrations steadily increased from 50 μg/m^3 to 120 μg/m^3. The four (4) periods represented different characteristics for the variability of $PM_{2.5}$ concentrations. P-1 showed a period that decreased in shape. P-2 indicated a period that accumulated heavy haze. P-3 represented a rapid cleaning process of the heavy haze, and P-4 suggested a heavy event that steadily increased.

The model calculation shows that the WRF-Chem model was capable of simulating a strong variability. The four (4) periods were well represented in the model calculation, indicating that the major factors, which affected the variability, were included in the model. As a result, the model result can be used to analyze the variability of the episode. However, we noticed some discrepancies between the modeled and measured results. For example, the measured maximum on Oct. 28 was underestimated by the calculation. As we will show in later sections, this underestimation is mainly due to a complex of meteorological conditions.

3.2 Effects of weather conditions on the haze

Weather maps of the episode were drawn (see Fig. 4). On Oct. 24, there was an anti-cyclone system with high air pressure (NW-High) located in the northwest of Beijing. This NW-High produced high northwest winds in the Beijing region, which was typical for producing low particle concentrations in Beijing. On Oct. 27, there was a weak system with very low winds in Beijing. This calm wind generally produced a concentration of high particles. On Oct. 28, Beijing was sandwiched between two (2) weather systems. In the northwest of Beijing, there was an anti-cyclone (NW-High), with north winds. In the southeast of Beijing, there was a cyclone (SE-Low), with southwest winds. Under these conditions, the particle pollutants in Beijing were trapped between the two (2) systems, leading to high pollution. On Oct. 29, the SE-Low in the south of Beijing retreated, and the anti-cyclone system with a high air pressure center located in the northwest of Beijing dominated. This was similar to the weather conditions on Oct. 24. As a result, the PM was rapidly transported to the downwind region of Beijing, leading to low pollution. The WRF-Chem model can further investigate the abovementioned effects of weather conditions on the $PM_{2.5}$ concentrations.

A horizontal distribution of $PM_{2.5}$ concentrations that corresponded to the different weather conditions was modeled (see Fig. 5). On Oct. 24, the $PM_{2.5}$ concentrations were low. The spatial distribution shows that the PM was largely diluted in the downwind region of Beijing due to high northwest winds. On Oct. 27, due to very weak winds, $PM_{2.5}$ concentrations strongly accumulated in Beijing City, resulting in a maximum of 400-500 $\mu g/m^3$ (hourly concentration at 8 a.m.) in Beijing City. On Oct. 28, the weather conditions were quite more complicated. First, the anti-cyclone was enhanced in the northwest of Beijing, generating northwest winds in the upwind region of Beijing. These conditions could have led to low $PM_{2.5}$ concentrations. However, there was also a cyclone system in the southeast of Beijing, which combined with south winds in the region. As a result, the $PM_{2.5}$ pollutants were sandwiched between the two (2) weather systems, producing a pollution belt and causing high $PM_{2.5}$ concentrations to be maintained in the Beijing region. As we can recall, the calculated $PM_{2.5}$ concentrations underestimated the measured values (see in fig. 3). One explanation for this is that under very complicated meteorological conditions, the regional model has some trouble reproducing small-scale meteorological features. Other reasons could include uncertainties in emissions, secondary aerosol formation, and so forth. On Oct. 29, the anti-cyclone in the northwest of Beijing was further enhanced, and more importantly, the cyclone in the south of Beijing retreated. As a result, strong northwest winds prevailed, and $PM_{2.5}$ was rapidly transported and diluted in the downwind region of Beijing, leading to the end of heavy $PM_{2.5}$ event that occurred during Oct. 27-28.

To understand the effects of weather conditions on $PM_{2.5}$ due to Beijing's local emissions, a model simulation is performed with Beijing emissions only. The surface distribution of $PM_{2.5}$ concentrations was calculated (see fig. 6). This calculation clearly shows that the $PM_{2.5}$ plumes originated from Beijing. On Oct. 24, the plumes moved southeast due to the strong northwest wind. On Oct. 27, the plumes became concentrated in Beijing, causing locally high $PM_{2.5}$ concentrations. This result also suggests that under calm wind conditions, the high $PM_{2.5}$ concentrations in Beijing were mainly affected by local emissions. On Oct. 28, the plumes were sandwiched by the NW-High and SE-Low, causing high $PM_{2.5}$ concentrations in the center and south of Beijing. On Oct. 29, the plumes were transported to the south with a strong dilution.

3.3 Correlation between $PM_{2.5}$ and important meteorological factors

The above analysis shows the overall relationship between weather systems and $PM_{2.5}$ concentrations, and does not provide detailed information regarding the effects of major meteorological factors associated with the weather systems on the $PM_{2.5}$ concentrations. In order to better understand the evolution of the haze events and the roles of major meteorological factors for the formation of hazes, the $PM_{2.5}$ concentrations and the corresponding meteorological factors were calculated, such as wind speed (WS), PBL height (PBLH), and a combination of the WS and PBLH, which is defined by the product of WS and PBLH (COMB = WS × PBLH) (see Fig. 7). All the WS and PBLH are daily averaged values, which were computed from hourly values. The results suggest that all three factors were strongly anti-correlated to the $PM_{2.5}$ concentrations. The correlation coefficients between $PM_{2.5}$ concentrations and the WS, the PBLH, and the COMB are -0.81, -0.86, and -0.78, respectively (see Fig. 7 and Fig. 8). It is worth noting that the correlation between $PM_{2.5}$ and the COMB has the lowest correlation. This is due to the fact that the relationship of $PM_{2.5}$-COMB has a non-linear curve as compared to $PM_{2.5}$-WS and $PM_{2.5}$-PBLH. At the low value of the COMB, the concentrations of $PM_{2.5}$ were very sensitive to the values of the COMB. For example, at the low side of the COMB, when the COMB values changed from 150 m^2/s to 500 m^2/s, the $PM_{2.5}$ concentrations rapidly reduced from 150 g/m^3 to 100 g/m^3. In contrast, at the high side of the COMB, when the COMB values changed from 4,000 m^2/s to 7,000 m^2/s, the $PM_{2.5}$ concentrations only reduced from 50 g/m^3 to 40 g/m^3. This result suggests that when both the WS and the PBLH are small, the COMB is very sensitive to the $PM_{2.5}$ concentrations. Any small changes of the COMB can lead to a large change in the $PM_{2.5}$ concentrations.

Due to the high correlations of $PM_{2.5}$-WS and $PM_{2.5}$-PBLH, the variability of $PM_{2.5}$ concentrations corresponded with the variability of the WS, the PBLH, and the COMB. For example, during the period between Oct. 24 and 27, the daily averaged $PM_{2.5}$ concentrations steadily increased from 40 to 170 $\mu g/m^3$. The corresponding WS decreased from 5 m/s to 1 m/s; the PBLH reduced from 1,200 m to 300 m, and the COMB declined from 6,000 m^2/s to 500 m^2/s. During the period between Oct. 29 and Oct. 31, the daily averaged $PM_{2.5}$ concentrations steadily increased from 50 to 150

μg/m^3. The corresponding WS decreased from 3.5 m/s to 1 m/s; the PBLH reduced from 1,000 m to 400 m; and the COMB declined from 2,500 m^2/s to 300 m^2/s. In addition to the winds and the PBLH, the relative humidity (RH) is also correlated to the haze events in Beijing (Zhang et al., 2014). Under high RH values, the hygroscopic growth of aerosol particles is significantly enhanced, leading to the reduction of visibility. This effect is out of the scope of this study.

3.4 Budget analysis

In order to use this simple box model for the budget analysis, Eq. (3) is first used to calculate the daily mean concentration during the heavy haze episode from Oct. 23 to 27 (see fig. 9). Three calculations were carried out with the following assumptions: (a) only primary $PM_{2.5}$ emissions are included. According to an estimation made by He et al. (2014), within 100 km × 100 km area that is centered in Beijing (as indicated in the black box in fig. 2), primary $PM_{2.5}$ emissions are 320 Kton/year in the Beijing region. The calculated result is shown by the green line; (b) secondary particles due to the formation of sulfate and nitrate was included in the calculation, with different percentages of gases (SO_2 and NO_x) to particles ($SO_4^=$ and NO_3^-) conversions. In addition to the inorganic secondary aerosol formation, there is also the formulation of secondary organic aerosol (SOA). As large uncertainty exists for estimating the formation of SOA, this issue is left for future studies. The surface emissions of SO_2 and NO_x are 210 Kton/year and 70 Kton/year in the 100 km × 100 km area, respectively. The black line represents that there is a 100% conversion between the gases and particles. In other words, both SO_2 and NO_x are released in the particle phase. When calculating, the PBLH, the WS, X_{in} and X_{out} are used to calculate the daily averaged values from the results of the WRF-Chem. The blue line represents that there is a 50% conversion between the gases and particles, namely, half of SO_2 and NO_x is released in the particle phase.

The results show that the calculations by the simple box model are capable of reproducing a large variability of the heavy haze event, but some discrepancies are also noticeable (see Fig. 9). From Oct. 23 to 25, the calculated $PM_{2.5}$ concentrations ranged from 40 to 60 μg/m^3) in the three cases, which were slightly higher than the measured values (25-45 μg/m^3). After Oct. 26, both the calculated and measured $PM_{2.5}$ concen-

trations rapidly increased. On Oct. 27, the calculated $PM_{2.5}$ concentrations ranged from 125-225 $\mu g/m^3$ in the three (3) cases, compared to the measured value of 155 $\mu g/m^3$. On Oct. 28, the calculated $PM_{2.5}$ concentrations reached to a maximum, ranging from 175-350 $\mu g/m^3$ in the three (3) cases, compared to the measured value of 255 $\mu g/m^3$. On Oct. 29, both the calculated and measured $PM_{2.5}$ concentrations rapidly decreased from the maximum. However, the measured value decreased in a more aggressive way than the calculated values. This calculation also suggests that with about 40% conversion between gases (SO_2 and NO_x) to particles ($SO_4^=$ and NO_3^-), the calculation performs better than the measured result.

Another important issue is that the PBLH and emissions have substantial diurnal variation. In the first one, we assume that the above box calculations use daily averaged values of the PBLH and emissions. In order to determine the effects of diurnal variability on the calculation, the results (see fig. 10) are recalculated with the following three (3) cases: (1) including the diurnal variation of PBLH only (PBLH-only), (2) including the diurnal variation of emissions only (EMIS-only), and (3) including both the diurnal variations of the PBLH and emissions (BOTH). The case containing the daily averaged values of the PBLH and emissions (see fig. 9) is also included in the figure. All calculations assumed 50% conversions between gas and aqueous phases. The result indicates that the diurnal variations of the PBLH and emissions have important effects on the calculated concentrations of $PM_{2.5}$. The PBLH-only calculation has a tendency to be higher than $PM_{2.5}$ concentrations, especially during haze days. In contrast, the EMIS-only calculation seems to be lower than the $PM_{2.5}$ concentrations. With the BOTH calculations, the overestimation (PBLH-only) and the underestimation (EMIS-only) balance each other. As a result, when using both the PBLH and emission variation, the calculated $PM_{2.5}$ concentrations are closer to the default calculation (the constant daily values of PBLH and emissions).

To understand the important processes controlling the formation of heavy haze better, several sensitive studies were performed by the box model. At first, we assumed that there was no horizontal dilution (a condition of calm winds), and the $PM_{2.5}$ continuously released into the city box. Eq. (3) can be rewritten as

$$[X]_{t+1} = [X]_t + \frac{EM}{PBLH} \times \Delta t \qquad (4)$$

We showed the temporal evolution of calculated $PM_{2.5}$ concentrations by applying Eq. (4) (see fig. 11). The results show that with continuous $PM_{2.5}$ emissions, the $PM_{2.5}$ concentrations increased linearly. This result also can provide a time scale for $PM_{2.5}$ to reach different haze levels. As no advection exists, the results provide the fastest time (upper limit) for the occurrences of haze events. For example, according to the results, for $PM_{2.5}$ concentrations reaching 150 $\mu g/m^3$, the time required for the accumulation of $PM_{2.5}$ emissions is 16 hours, 24 hours, and 32 hours, with 100%, 40%, 0% gas to particle conversions, respectively. For $PM_{2.5}$ concentrations reaching to 250 $\mu g/m^3$, the time required due to $PM_{2.5}$ emissions is 32 hours and 44 hours with 100% and 40% gas to particle conversions, respectively. If we use 40% as a standard calculation, within one (1) day, the $PM_{2.5}$ concentrations can reach 150 $\mu g/m^3$, and within two (2) days, the $PM_{2.5}$ concentrations can reach 250 $\mu g/m^3$. The PBL height was set-up to be 1,000 m for all the above calculations.

Eq. (4) also assumes that the $PM_{2.5}$ emissions are vertically mixed inside the PBL heights. As a result, the $PM_{2.5}$ concentrations are very sensitive to the PBLH. To study the sensitivity of the $PM_{2.5}$ concentrations to the PBL heights, we used Eq. (4) with the following conditions: 40% gas to particle conversions and 36 hours of Δt. The calculated result suggests that $PM_{2.5}$ concentrations are very sensitive to the PBL heights. The calculated $PM_{2.5}$ concentrations of 200 $\mu g/m^3$, 350 $\mu g/m^3$, and 600 $\mu g/m^3$, correspond to the PBL heights of 1,000 m, 500 m, and 300 m, respectively (see Fig. 12). More importantly, the relationship between $PM_{2.5}$ concentrations and PBL heights is non-linear. For example, the ratio between $PM_{2.5}$ concentrations and PBL heights (Rp = $\Delta[PM_{2.5}]/\Delta[PBL]$) is 0.12 $\mu g/m^4$ for the PBL heights of 1,200 m. However, when the PBL heights reduced to 300 m, the ratio of Rp enhanced to 2.2 $\mu g/m^4$. This rapid increase in the ratio suggests that at lower PBL heights, the $PM_{2.5}$ concentrations are extremely sensitive to the PBL heights, and any small changes in PBL heights could lead to significant changes in $PM_{2.5}$ concentrations.

The next analysis is to understand the city limit of atmospheric pollutants. From the expression of the mass balance equations (2) and (3), when the emissions of pollu-

tants is balanced by such removal processes (transport and diffusion), it can be expressed by

$$\frac{EM}{PBLH} + \{(WS \times [X])_{in} - (WS \times [X])_{out}\}/DL = 0 \qquad (5)$$

The wind speed (WS) for reaching the balance can be expressed by

$$WS_b = \left(\frac{EM}{PBLH}\right) / \{([X])_{out} - [X])_{in})/DL\} \qquad (6)$$

The WS_b is the expression for the required wind speed to reach a balance between continuous emissions and atmospheric cleaning processes. The physical meaning of WS_b can be expressed by:

(a) $WS < WS_b$: PM concentrations increase (an accumulation mode)
(b) $WS = WS_b$: PM concentrations remain constant (a neutral mode)
(c) $WS > WS_b$: PM concentrations decrease (a cleaning mode)

In calculating, the 40% gas to particle phase conversions for both SO_2 and NO_x are assumed according to the calculation shown (see Fig. 1). The $[X]_{out}$ is set at 200 $\mu g/m^3$ for presenting pollution. The two $[X]_{in}$ values (20 $\mu g/m^3$ and 100 $\mu g/m^3$) are applied in the calculation. With northwesterly wind, the upwind regions of Beijing are relatively clean of PM (as shown in Fig. 2), and the value of 20 $\mu g/m^3$ is used for $[X]_{in}$. In contrast, with southerly wind, the upwind regions of Beijing are relatively dirty, and the value of 100 $\mu g/m^3$ is used to present a polluted regional backdrop.

Eq. (6) also shows that the value of WS_b is sensitive to the PBL height. The WS_b under different PBL heights is calculated (see Fig. 13). The results show that the WS_b values strongly vary with the PBL heights. In the case of 20 $\mu g/m^3$ for $[X]_{in}$, when the PBL heights are higher than 700 m, the variation of WS_b is small (close to 1 m/s). This result implies that under the NW-high and relatively high PBL conditions, the PM can be easily cleaned by advection, and PM will hardly accumulate to form haze. The WS_b rapidly increases when the PBL heights are lower than 400 m. For example, the WS_b values are 2.5 m/s and 4.0 m/s with the PBL heights of 300 m and 200 m,

503 respectively. This result suggests that when the prevailing wind in Beijing is a north-
504 west wind (the NW-High condition) and the wind speed is greater than 4 m/s, the PM
505 is under a cleaning mode. This general conclusion excludes the extreme case that
506 when the PBL heights are very low (100 m), it requires the wind speed of 7.8 m/s to
507 switch from the accumulation mode to the cleaning mode.
508
509 In the case of 100 μg/m^3 for $[X]_{in}$ under an SE-Low, the required wind speed to switch
510 from the accumulation mode to the cleaning mode is significantly higher than the first
511 case. For example, when the PBL heights are higher than 700 m, the values of the
512 WS_b is about 2 m/s. With a shallower PBL, a higher wind speed is needed to switch
513 from the accumulation mode to the cleaning mode. For instance, the values of the
514 WS_b are 4.5 m/s and 7 m/s, with the PBL heights of 300 m and 200 m, respectively.
515 Under the extreme case of 100 m for the PBL heights, it requires the wind speed of
516 13.6 m/s to switch the PM from the accumulation mode to the cleaning mode. This
517 result suggests that when the prevailing wind is a south wind (under the SE-Low con-
518 dition), the required wind speed needed to switch the PM from the accumulation
519 mode to the cleaning mode is very high, especially under low PBL conditions.
520
521 **4. Summary**
522
523 In recent times, high $PM_{2.5}$ concentrations have often occurred during the winter,
524 causing a serious haze problem in Beijing. To study this "Beijing Haze", a haze epi-
525 sode (from Oct. 21 to Oct. 31, 2013) in Beijing was analyzed. During the episode, the
526 daily mean concentration of $PM_{2.5}$ reached a peak value of 250 μg/m^3 on Oct. 28,
527 2013, and rapidly decreased to 50 μg/m^3 the next day (Oct. 29, 2013). With a large
528 and rapid variability, the high $PM_{2.5}$ concentrations have provided a good opportunity
529 to study the causes of the formation of the haze. In this study, two numerical models
530 were applied. The first model was a chemical/dynamical regional model (WRF-
531 Chem), which was mainly used to study the regional effects of weather conditions on
532 $PM_{2.5}$ concentrations in the Beijing region. The second model was a simplified box
533 model, which was applied to estimate some crucial parameters regarding the PM in
534 the Beijing region. The main findings of this study are summarized as follows:
535
536 (1)The city of Beijing is in a special geographical location. In the northwest area of

Beijing, there are mountains and grasslands, with a very small population. As a result, the northwest wind transports clean air to Beijing. In contrast, in the south of Beijing, the population is very dense, with several mega/large cities. Thus, the south wind transports polluted air to Beijing. Within this particular geographical location, weather conditions majorly influence the formation of haze in Beijing. When a high air pressure system appears in northwest Beijing (NW-High), it generally produces strong northwest winds with clean upwind air. As a result, the NW-High plays an important role in cleaning the PM in Beijing. However, when there is a low air pressure in southeast Beijing (SE-Low) accompanied with a NW-High, an air convergent zone occurs in Beijing. The pollutants are sandwiched between the two (2) systems, producing high $PM_{2.5}$ concentrations in the Beijing region.

(2)The $PM_{2.5}$ concentrations are significantly affected by local meteorological factors, such as wind speed (WS), PBL height (PBLH), and a combination of the WS and the PBLH, which is defined by the product of the WS and the PBLH (COMB = WS × PBLH). The correlation coefficients between $PM_{2.5}$ concentrations and the WS, the PBLH, and the COMB are -0.81, -0.86, and -0.78, respectively. There is a non-linear correlation between the $PM_{2.5}$ concentrations and PBLH\COMB, while the correlation between the $PM_{2.5}$ concentrations and WS is nearly linear.

(3)The budget analysis shows that with calm winds and continuous surface emissions, the daily mean $PM_{2.5}$ concentrations can reach 150 $\mu g/m^3$ within one (1) day, and 250 $\mu g/m^3$ within two (2) days. This suggests that the current emission levels are high and can easily cause the formation of hazes.

(4)The wind speed for reaching a balance between continuous emissions and atmospheric clean processes (WS_b) is studied. The result shows that WS_b is strongly dependent on the PBL height and the wind direction. Under an SE-Low, the WS_b is 2 m/s with a higher PBL height (700 m). However, under lower PBL heights, the WS_b rapidly increases, reaching 4.5 m/s and 7.0 m/s, with PBL heights of 300 m and 200 m, respectively. In contrast, under a NW-High, the WS_b reduces to 2.5 m/s and 4.0 m/s. This result suggests that when the prevailing wind in Beijing is a northwest wind (with a wind speed of > 4 m/s), the PM is under a cleaning mode.

ACKNOWLEDGMENTS: This research is partially supported by the National Natural Science Foundation of China (NSFC) under Grant Nos. 41275186, 41430424, 41175007, and 41375135. The National Center for Atmospheric Research is sponsored by the National Science Foundation.

References

Bian H., S. Q. Han, X. Tie, M. L. Shun, and A. X. Liu, Evidence of Impact of Aerosols on Surface Ozone Concentration: A Case Study in Tianjin, China, *Atmos. Environ., 41, 4672-4681,* 2007.

Binkowski, F. S. and Roselle, S. J., Models-3 Community Multiscale Air Quality (CMAQ) model aerosol component: 1. Model description, *J. Geophys. Res., 108(D6),* 4183, doi:10.1029/2001JD001409, 2003.

Cao, J. J., Q. Y. Wang, J. C., Chow, J. G. Watson, X. Tie, Z. X. Shen, P. Wang, Z. S. An, Impacts of aerosol compositions on visibility impairment in Xi'an, China. *Atmos. Environ., 59,* 559-566, DOI: 10.1016/j.atmosenv.2012.05.036, 2012

Cao J. J., X. Tie, W. Dabberdt, Z. Z. Zhao, and T. Jie, On potential acid rain enhancement in eastern China, *J. Geophys. Res., 118,* 4834–4846, doi:10.1002/jgrd.50381, 2013.

Chan, C. K., Yao, X., Air pollution in megacities in China. *Atmos. Environ. 42(1),* 1–42, 2008.

Chang, J. S., Binkowski, F. S., Seaman, N. L., McHenry, J. N., Samson, P. J., Stockwell, W. R., Walcek, C. J., Madronich, S., Middleton, P. B., Pleim, J. E., and Lansford, H. H., The regional acid deposition model and engineering model, State-of-Science/Technology, Report 4, *National Acid Precipitation Assessment Program*, Washington DC, 1989.

Chen, F. and Dudhia, J., Coupling an advanced land-surface/hydrology model with the Penn State/NCARMM5 modeling system. Part I: Model description and implementation, *Mon. Weather Rev., 129,* 569–585, 2001.

Deng X. J, X. Tie, D. Wu, X. J. Zhou, H. B. Tan, F. Li, C. Jiang, Long-term trend of visibility and its characterizations in the Pearl River Delta Region (PRD), China, *Atmos. Environ., 42,* 1424-1435, 2008.

Dudhia, J., Numerical study of convection observed during the winter monsoon experiment using a mesoscale two-dimensional model, *J. Atmos. Sci., 46,* 3077–3107, 1989.

Emmons, L. K., S. Walters, P. G. Hess, J.-F. Lamarque, G. G. Pfister, D. Fillmore, C. Granier, A. Guenther, D. Kinnison, T. Laepple, J. Orlando, X. Tie, G. Tyndall, C. Wiedinmyer, S. L. Baughcum, and S. Kloster, Description and evaluation of the Model for Ozone and Related chemical Tracers, version 4 (MOZART-4), *Geosci. Model Dev., 3,* 43-67, 2010.

Grell, G. A., Peckham, S. E., Schmitz, R., McKeen, S. A., Wilczak, J., and Eder, B.: Fully coupled "online" chemistry within the WRF model, *Atmos. Environ., 39,* 6957–6975, 2005.

Guinot, B., Cachier, H., J., Sciare, Yu, T., Wang X., Yu J.H., Beijing aerosol: atmospheric interactions and new trends. *J. Geophys. Res. 112* (D14314), doi:10.1029/2006JD008195, 2007.

He H., X. Tie, Q. Zhang, X. Liu, Q. Gao, X. Li, and Y. Gao, Analysis of the causes of heavy aerosol pollution in Beijing, China: A case study with the WRF-Chem model, *Particuology*, in press, 2014.

He, K. B., Yang, F., Ma, Y. L., Zhang, Q., Yao, X. H., Chan, C. K., Cadle, S., Chan, T., Mulawa, P., The characteristics of PM2.5 in Beijing, China. *Atmos. Environ. 35*, 4959–4970, 2001.

Li, G., Zavala, M., Lei, W., Tsimpidi, A. P., Karydis, V. A., Pandis, S. N., Canagaratna, M. R., and Molina, L. T., Simulations of organic aerosol concentrations in Mexico City using the WRF- CHEM model during the MCMA-2006/MILAGRO campaign, *Atmos. Chem. Phys., 11,* 3789–3809, doi:10.5194/acp-11-3789- 2011, 2011.

Lin, Y.-L., Farley, R. D., and Orville, H. D., Bulk parameterization of the snowfield in a cloud model, *J. Appl. Meteorol., 22*, 1065–1092, 1983.

Madronich, S. and Flocke, S., The role of solar radiation in atmospheric chemistry, in: *Handbook of Environmental Chemistry*, edited by: Boule, P., Springer-Verlag, Heidelberg, 1–26, 1999.

Martin, R. V., Jacob, D. J., Yantosca, R. M., Chin, M., and Ginoux, P., Global and regional decreases in tropospheric oxidants from photochemical effects of aerosols, J. Geophys. Res., 108(D3), 4097, doi:10.1029/2002JD002622, 2001.

Noh, Y., Cheon, W. G., and Raasch, S., The improvement of the K- profile model for the PBL using LES. Preprints, Int. Workshop of Next Generation NWP Models, Seoul, South Korea, *Laboratory for Atmospheric Modeling Research*, 65–66, 2001.

Quan, J., Gao, Yang., Q. Zhang, X. Tie, J. J. Cao, S. Q. Han, J. W. Meng, P. F. Chen, D. L. Zhao, Evolution of the planetary boundary layer under different weather conditions, and its impact on aerosol concentrations. *Particuology*, doi: 10.1016/j.partic.2012.04.005, 2013.

Skamarock, W. C., J. B. Klemp, J. Dudhia, D. O. Gill, D. M. Barker, M. G. Duda, X. Y. Huang, W. Wang, J. G. Powers, A description of the advanced research WRF version 3, NCAR Technical Note (NCAR/TN-475+STR), 2008.

Streets, D. G., Bond, T. C., Carmichael, G. R., Fernandes, S. D., Fu, Q., He, D., Klimont, Z., Nelson, S.M., Tsai, N.Y., Wang, M.Q., Woo, J.-H., Yarber, K.F., An inventory of gaseous and primary aerosol emissions in Asia in the year 2000. *J. Geophys. Res., 108,* 8809, 2003.

Streets, D.G., C. Yu, Y. Wu, M. Chin, Z. Zhao, T. Hayasaka, G. Shi, Aerosol trends over China, 1980-2000, *Atmos. Res., 88*, 174-182, 2008.

669 Tie, X., G. Brasseur, L. Emmons, L. Horowitz, and D. Kinnison, Effects of aerosols
670 on tropospheric oxidants: A global model study, *J. Geophys. Res.***,** *106*, 22931-
671 22964, 2001.
672
673 Tie, X., Madronich, S., Walters, S., Rasch, P., and Collins, W.: Effect of Clouds on
674 photolysis and oxidants in the troposphere, *J. Geophys. Res.*, *108*, 4642,
675 doi:10.1029/2003JD003659, 2003.
676
677 Tie, X., S. Madronich, S. Walters, D.P. Edwards, P. Ginoux, N. Mahowald, R.Y.
678 Zhang, C. Lou, and G. Brasseur, Assessment of the global impact of aerosols on
679 tropospheric oxidants, *J. Geophys. Res.*, *110* (D03204),
680 doi:10.1029/2004JD005359, 2005
681
682 Tie, X., Madronich, S., Li, G. H., Ying, Z. M., Zhang, R., Garcia, A., Lee-Taylor, J.,
683 and Liu, Y., Characterizations of chemical oxidants in Mexico City: A regional
684 chemical/dynamical model (WRF-Chem) study, *Atmos. Environ.*, *41*, 1989–2008,
685 2007.
686
687 Tie, X., D. Wu, and G. Brasseur, Lung Cancer Mortality and Exposure to Atmospher-
688 ic Aerosol Particles in Guangzhou, China, *Atmos. Environ.*, *43*, 2375–2377, 2009.
689
690 Tie X., F. Geng, A. Guenther, J. Cao, J. Greenberg, R. Zhang, E. Apel, G. Li,
691 A. Weinheimer, J. Chen, and C. Cai**,** Megacity impacts on regional ozone for-
692 mation: observations and WRF-Chem modeling for the MIRAGE-Shanghai field
693 campaign, *Atmos. Chem. Phys.*, *13***,** 5655-5669, doi:10.5194/acp-13-5655-2013,
694 2013.
695
696 Wesely, M. L.: Parameterization of surface resistance to gaseous dry deposition in re-
697 gional-scale numerical models, *Atmos. Environ*., 23, 1293–1304, 1989.
698
699 Yang, F., Tan, J., Zhao, Q., Du, Z., He, K., Ma, Y., Duan, F., Chen, G., Characteris-
700 tics of PM2.5 speciation in representative megacities and across China, *Atmos.*
701 *Chem. Phys. 11*, 5207-5219, 2011.
702
703 Zhang, Q., C. Zhao, X. Tie, Q. Wei, G. Li, and C. Li, Characterizations of Aerosols
704 over the Beijing Region: A Case Study of Aircraft Measurements, *Atmos. Envi-*
705 *ron.*, 40, 4513-4527, 2006.
706
707 Zhang, Q., XC. Ma, X. Tie, MY. Huang, and CS., Zhao, Vertical Distributions of Aer-
708 osols under Different Weather Conditions; Analysis of In-situ Aircraft Measure-
709 ments in Beijing, China, *Atmos. Environ. 9*, 4621-4638, 2009.
710
711 Zhang, Q., J. N. Quang, X. Tie, X. Li, Q. Liu, Y. Gao, and DL Zhao, Effects of mete-
712 orology and secondary particle formation on visibility during heavy haze events
713 in Beijing, China, *Sci. of Total Environ*., submitted, 2014.
714
715 Zhang R., J. Jing, J. Tao, S.-C. Hsu, G. Wang, J. Cao, C. S. L. Lee, L. Zhu, Z. Chen,
716 Y. Zhao, and Z. Shen, Chemical characterizations and source apportionment of
717 PM2.5 in Beijing: Seasonal perspective, *Atmos. Chem. Phys.* 13, 7053–7074,
718 doi:10.5194/acp-13-7053-2013, 2013.

Figure Captions

Figure 1. A schematic picture of the 100 km ×100 km horizontal box representing Beijing. The vertical height of the box is the PBL height. The surface emissions of the primary $PM_{2.5}$ and SO_2+NO_x are 320 and 270 Kton/year, respectively.

Figure 2. Average hourly emissions of $PM_{2.5}$ (g/s) in Beijing City and its surrounding regions, which are used in the model calculation. The black box shows a 100 km ×100 km domain centered in Beijing. The white and black arrows represent the northwest and south/southeast winds, respectively.

Figure 3. The calculated (green bars) and measured (red bars) daily mean $PM_{2.5}$ concentrations in a pollution episode from Oct. 21 to Oct. 23, 2013 in Beijing. The P-1, P-2, P-3, and P-4 indicates different periods, with different variability of $PM_{2.5}$ concentrations.

Figure 4. The weather maps during the pollution episode. On Oct. 24, there was an anti-cyclone system with a high air pressure (NW-High) located in northwest of Beijing. On Oct. 27, there was a weak system with very low winds in Beijing. On Oct. 28, Beijing was located between two (2) weather systems. In the northwest of Beijing, there was an anti-cyclone (NW-High), and in the southeast of Beijing, there was a cyclone (SE-Low), with southwest winds. On Oct. 29, the SE-Low in south of Beijing retreated, and the anti-cyclone system with a high air pressure center located in the northwest of Beijing dominated.

Figure 5. The modeled horizontal distribution of $PM_{2.5}$ concentrations ($\mu g/m^3$) corresponding to different weather conditions (see fig. 3).

Figure 6. Same as Fig. 5, except that emissions in the surrounding areas are excluded, and only local emissions in Beijing are used in the model.

Figure 7. The calculated $PM_{2.5}$ concentrations (purple bars) and the corresponding meteorological factors, such as wind speed (green bars), PBL heights (blue bars),

and a combination of the WS and PBLH, which is defined by the product of the WS and the PBLH (brown bars).

Figure 8. Dispersion plots and correlation coefficients between $PM_{2.5}$ concentrations and the WS (green dots), the PBLH (blue dots), and the COMB (brown dots). The values of coefficients are -0.81, -0.86, and -0.78, respectively.

Figure 9. The calculated daily mean concentration during the heavy haze episode from Oct. 23 to 29 using the box model. Three model calculations with different percentages of gases (SO_2 and NO_x) to the conversion of particles ($SO_4^=$ and NO_3^-) are performed, including (a) 100% (black line), (b) 50% (blue line), and (c) 0% (green line). The red line represents the measured result.

Figure 10. The calculated daily mean concentration during the heavy haze episode from Oct. 23 to 29 using the box model. Four model calculations with different diurnal variations: (1) including the diurnal variation of PBLH only (blue line), (2) including the diurnal variation of emissions only (green line), (3) including both the diurnal variations of the PBLH and emissions (black line), and (4) daily averaged values of the PBLH and emissions (red line). All calculations assume 50% conversions between gas and aqueous phases,

Figure 11. The calculated evolution of $PM_{2.5}$ concentrations under calm wind conditions. Three model calculations with different percentages of gases (SO_2 and NO_x) to the conversion of particles ($SO_4^=$ and NO_3^-) are performed: (1) 100% (green line), (2) 40% (red line), and (3) 0% (blue line). The triangles show the calculated concentration levels at 150 and 250 $\mu g/m^3$.

Figure 12. The variation of calculated $PM_{2.5}$ concentrations with different PBL heights, under calm winds.

Figure 13. The calculated values of the WS_b (the required wind speed to reach a balance between continuous emissions and atmospheric clean processes) at different PBL heights. The blue line and red line represent the northwest and south wind directions, respectively.

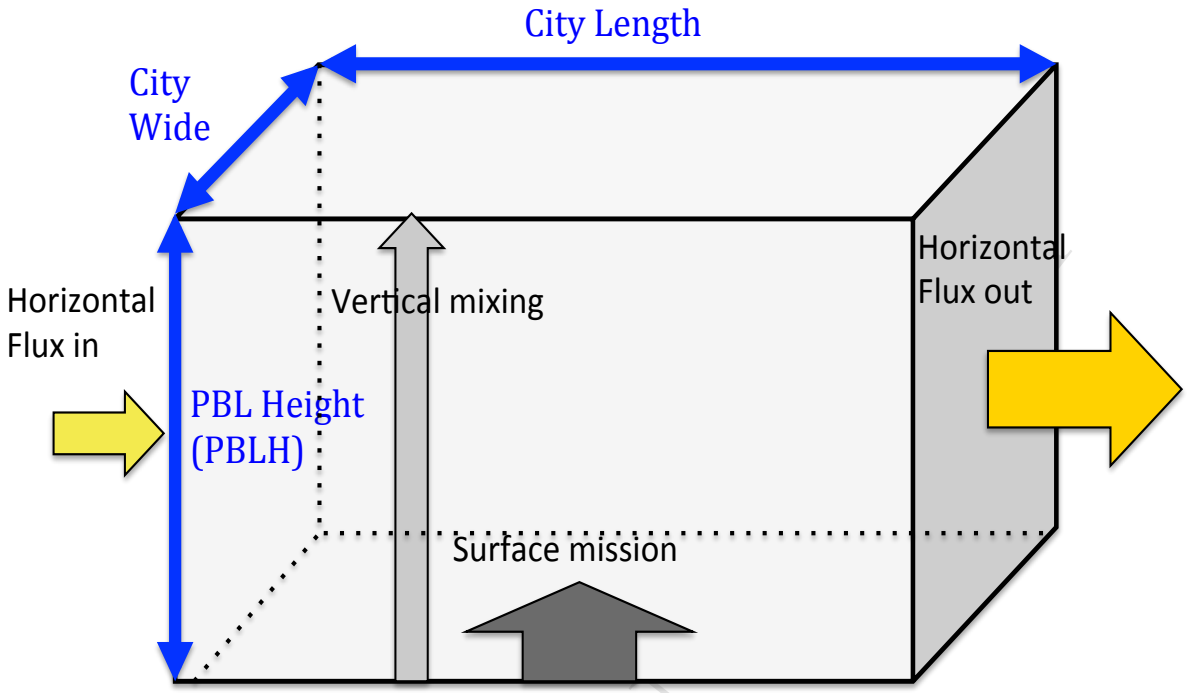

The city length = 100 km
The city wide = 100 km
$PM_{2.5}$ particle emission rate = 320 kton/year
SO_2 and NOx emission rate = 270 kton/year

F1

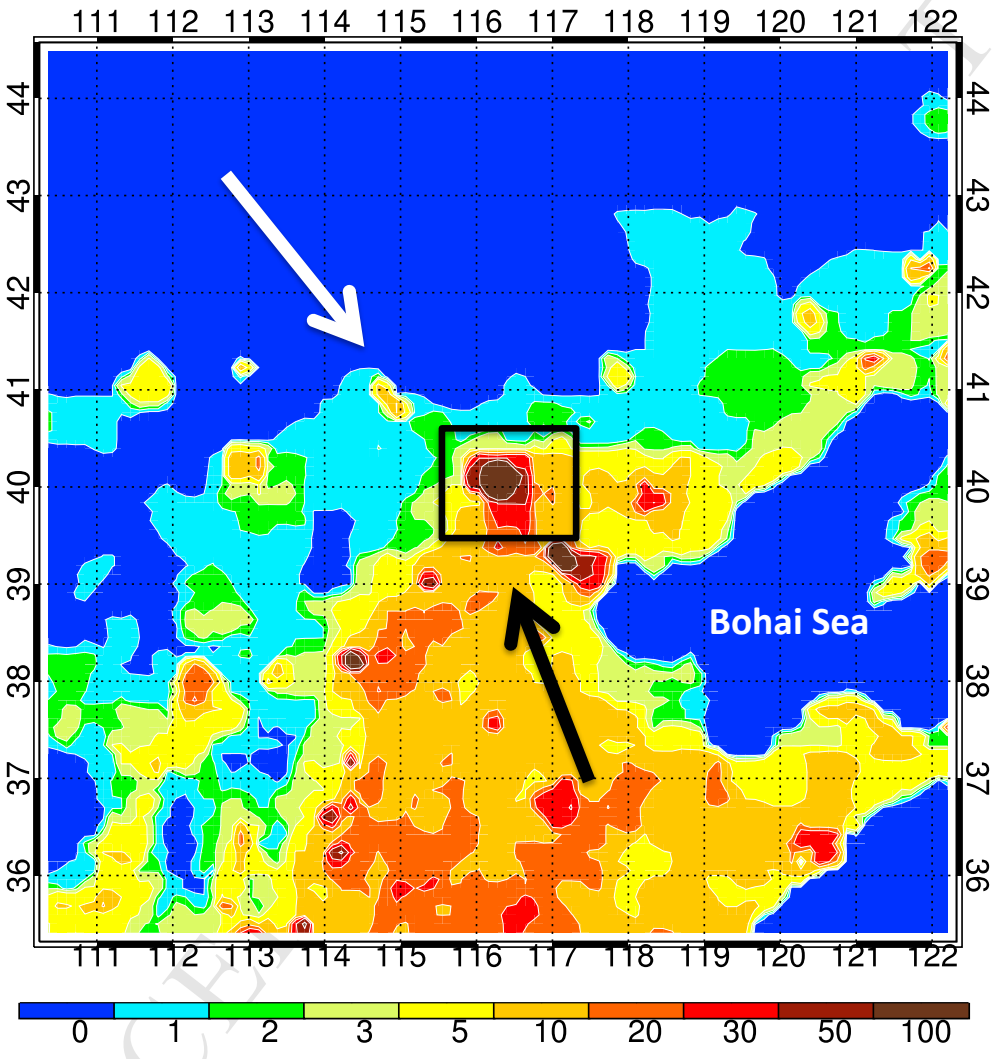
111 112 113 114 115 116 117 118 119 120 121 122
44 43 42 41 40 39 38 37 36
Bohai Sea
0 1 2 3 5 10 20 30 50 100
PM2.5 emis (g/s)

F2

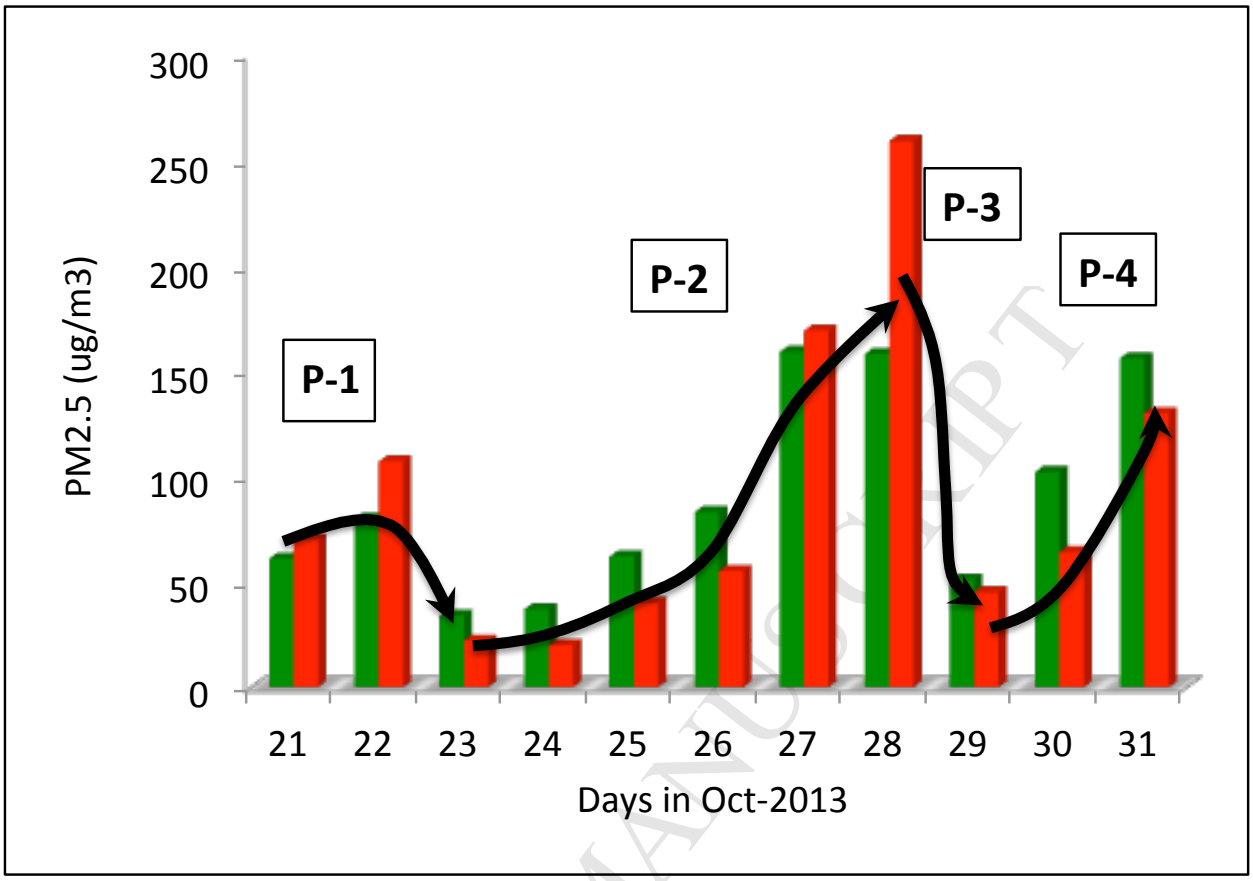

F3

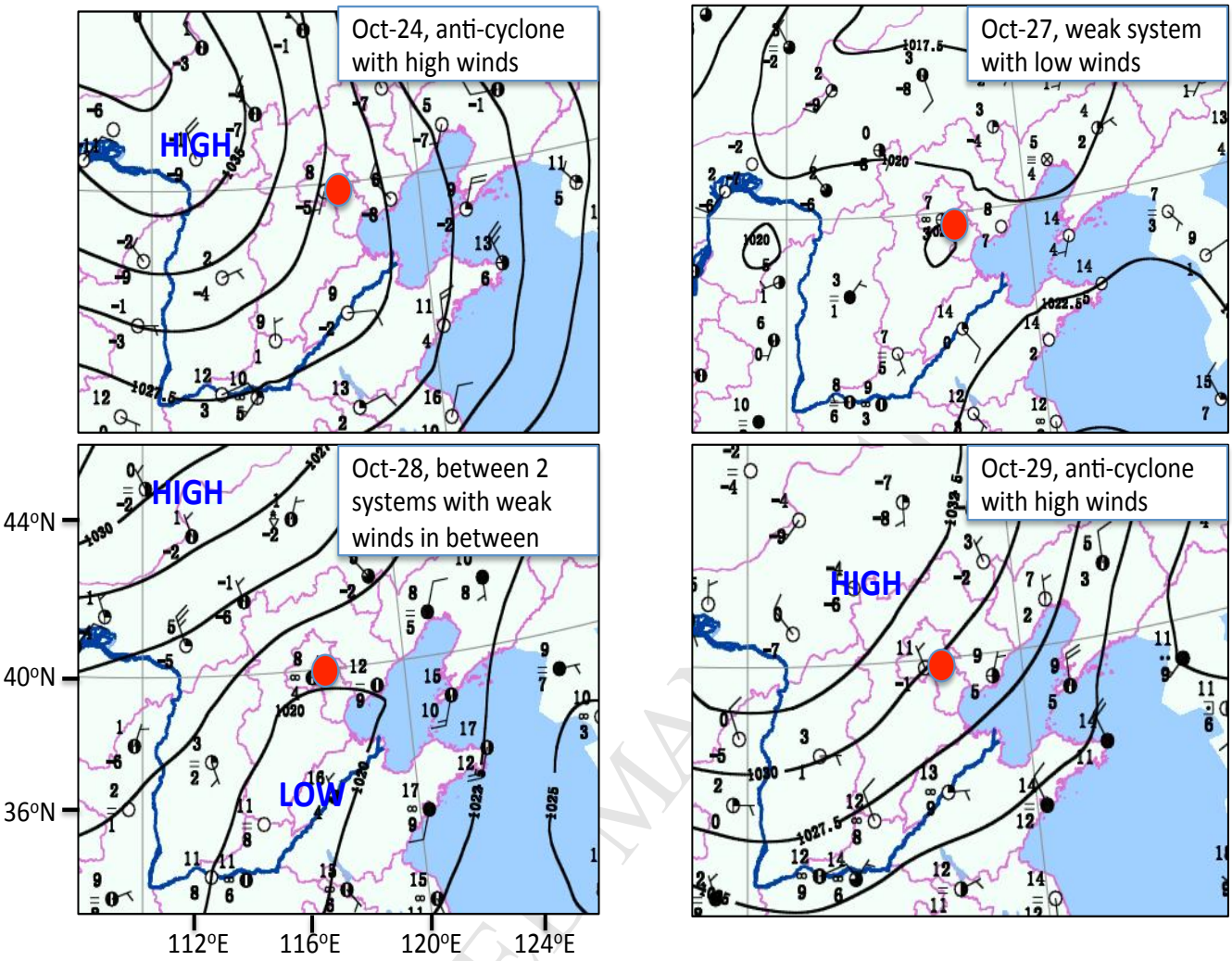

F4

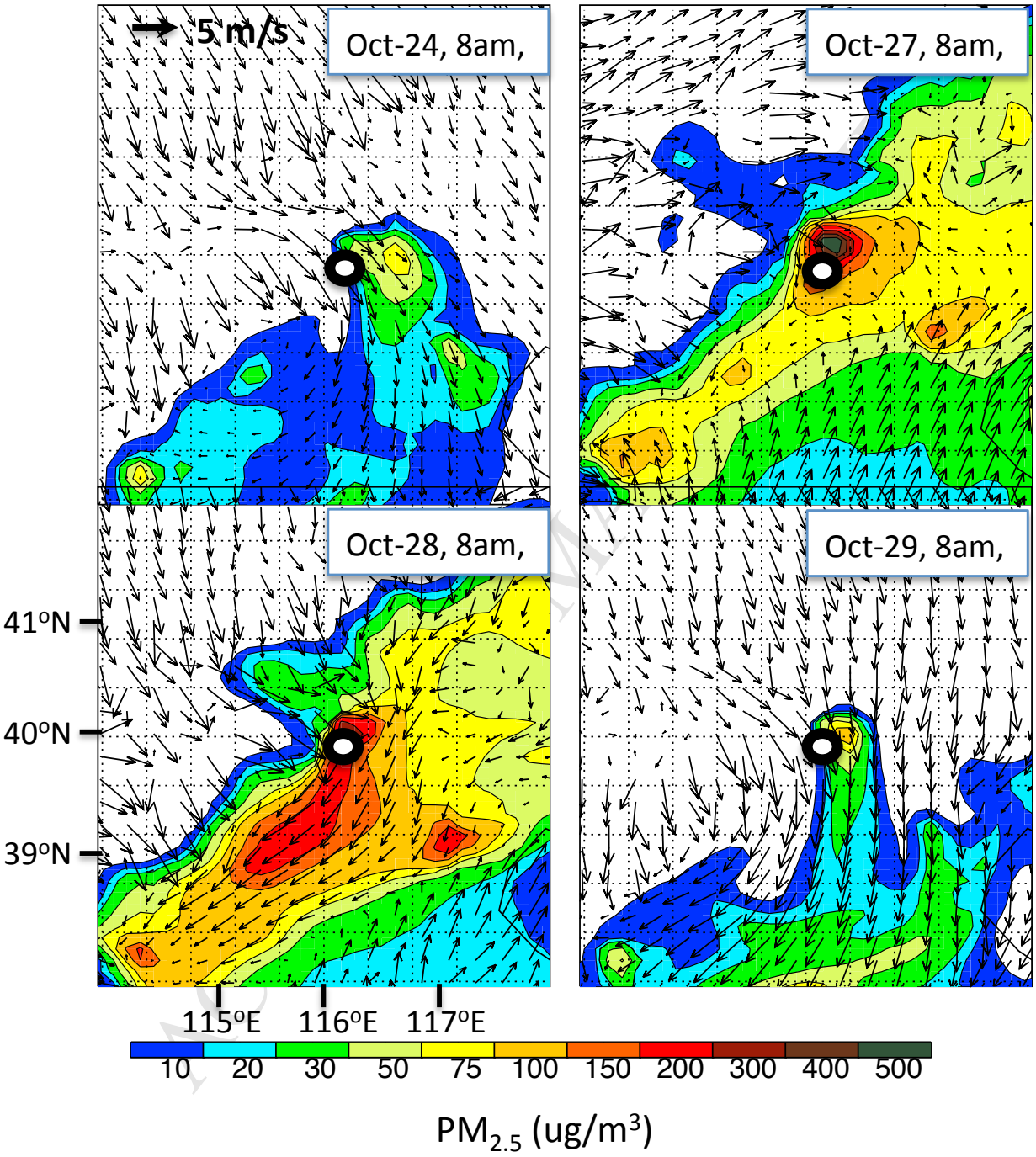
5 m/s
Oct-24, 8am,
Oct-27, 8am,
Oct-28, 8am,
Oct-29, 8am,
41°N
40°N
39°N
115°E
116°E
117°E
10
20
30
50
75
100
150
200
300
400
500
PM2.5 (ug/m3)

F5

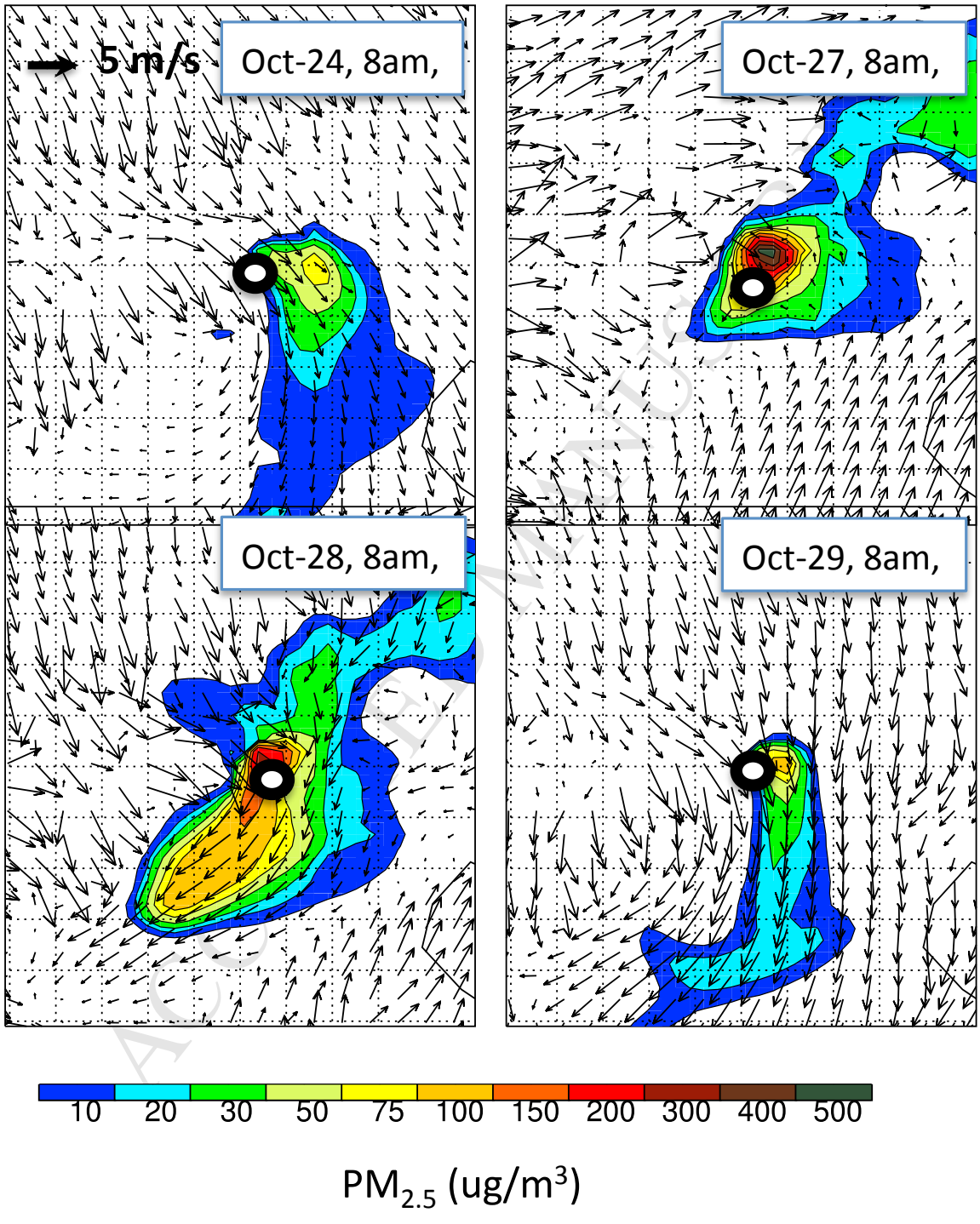
5 m/s
Oct-24, 8am,
Oct-27, 8am,
Oct-28, 8am,
Oct-29, 8am,
10
20
30
50
75
100
150
200
300
400
500
PM2.5 (ug/m3)

F6

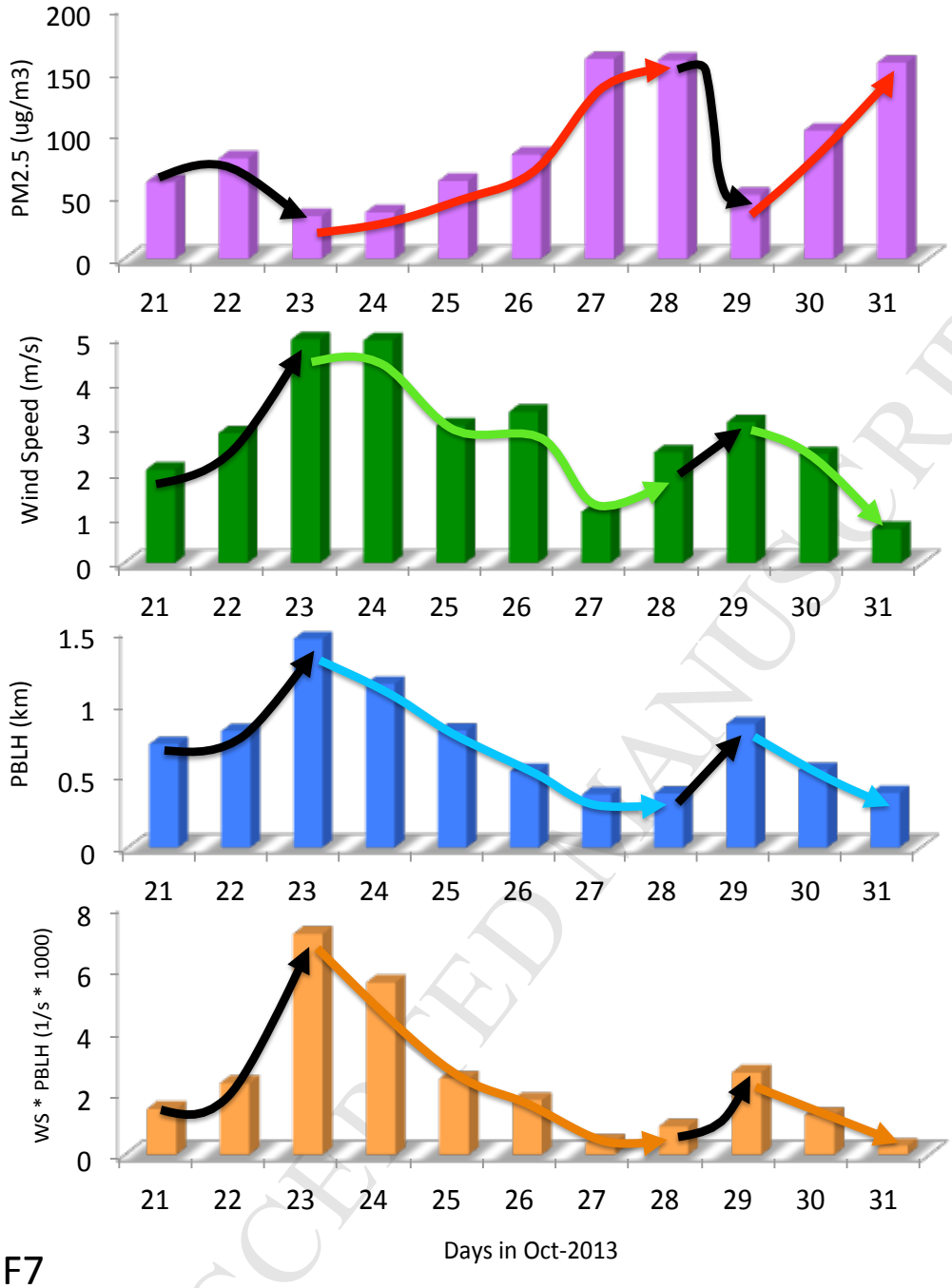

F7

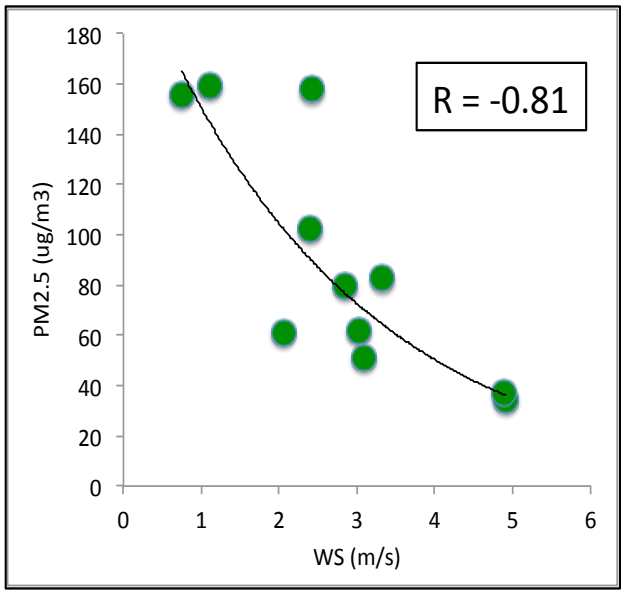

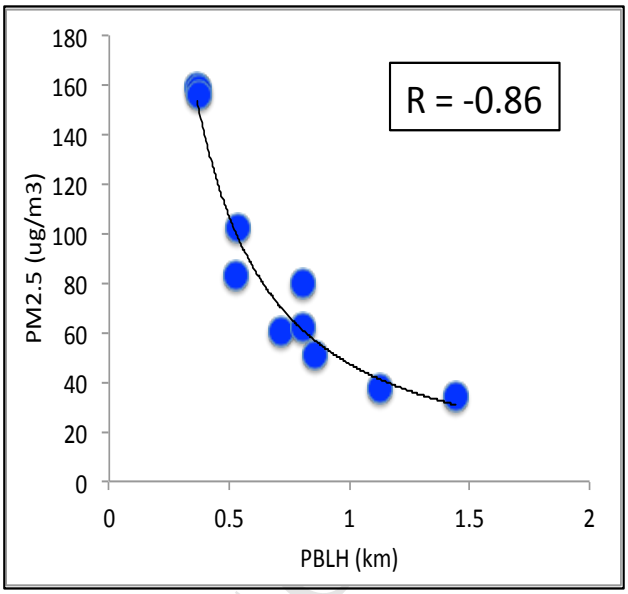

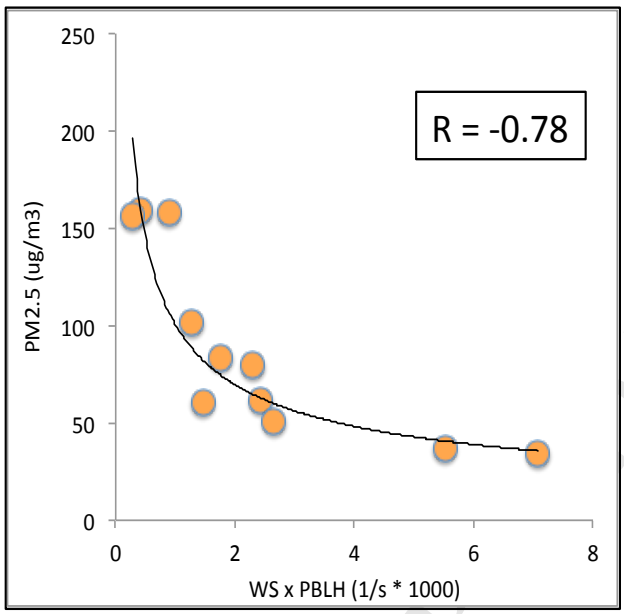

F8

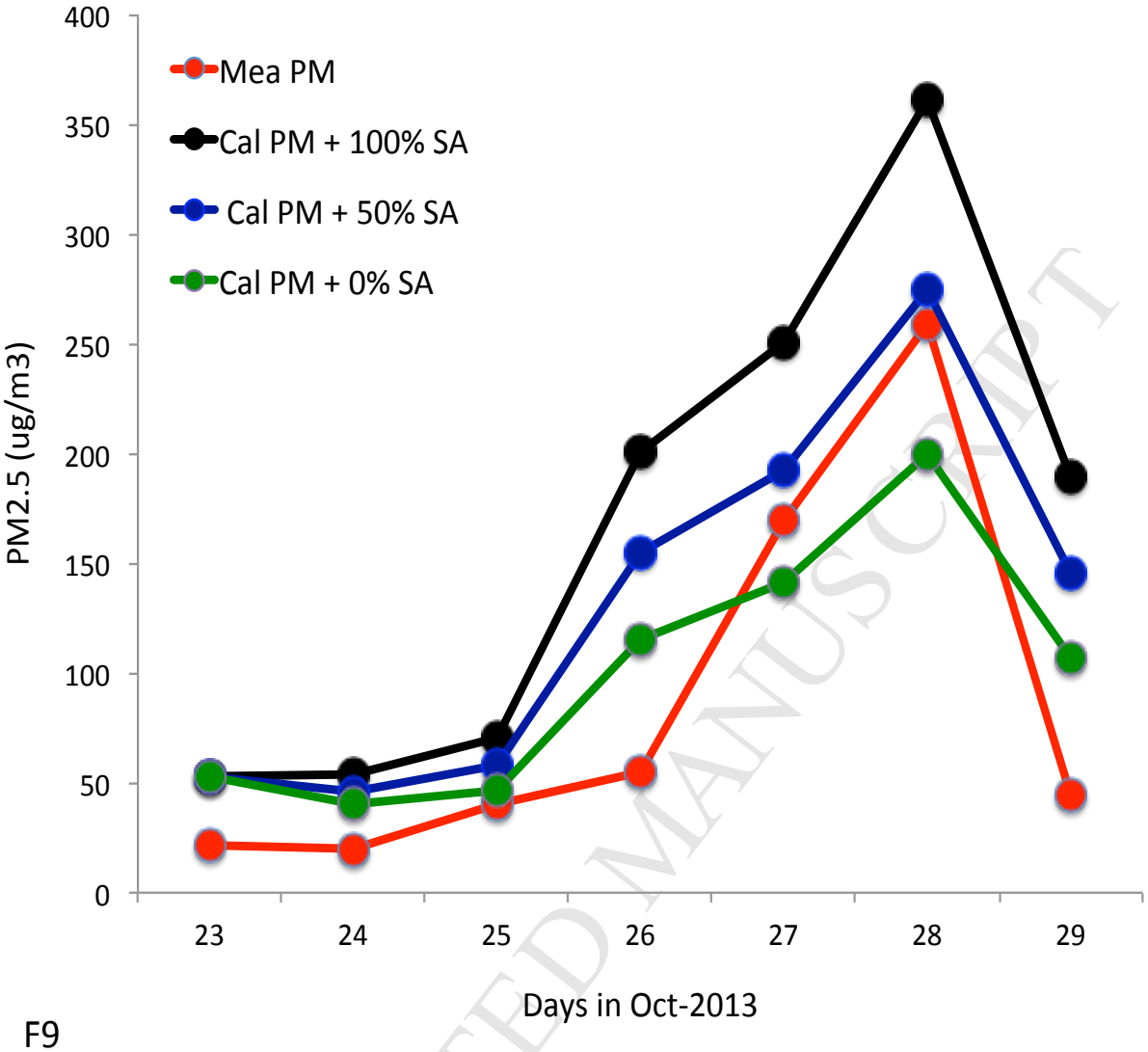

F9

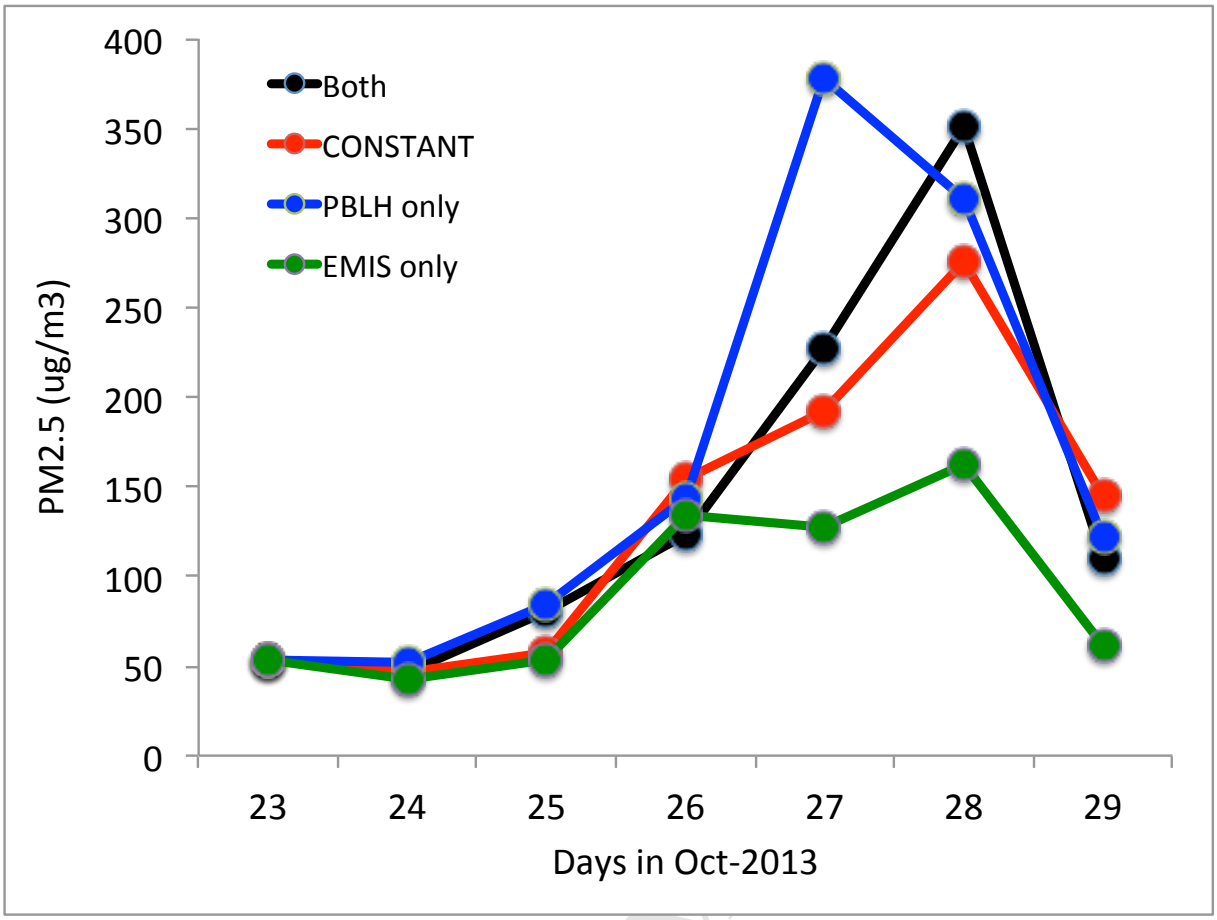

F10

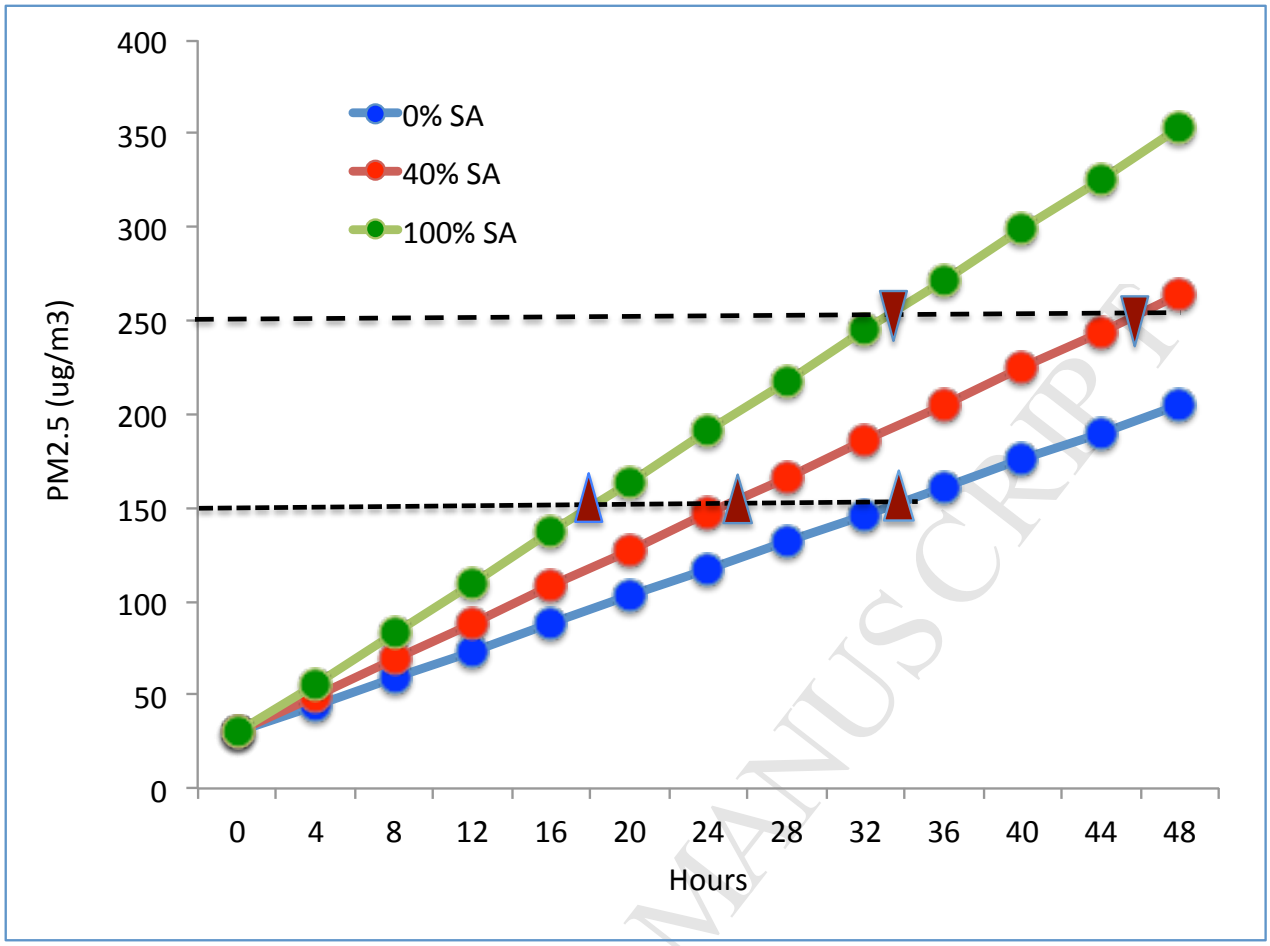

F11

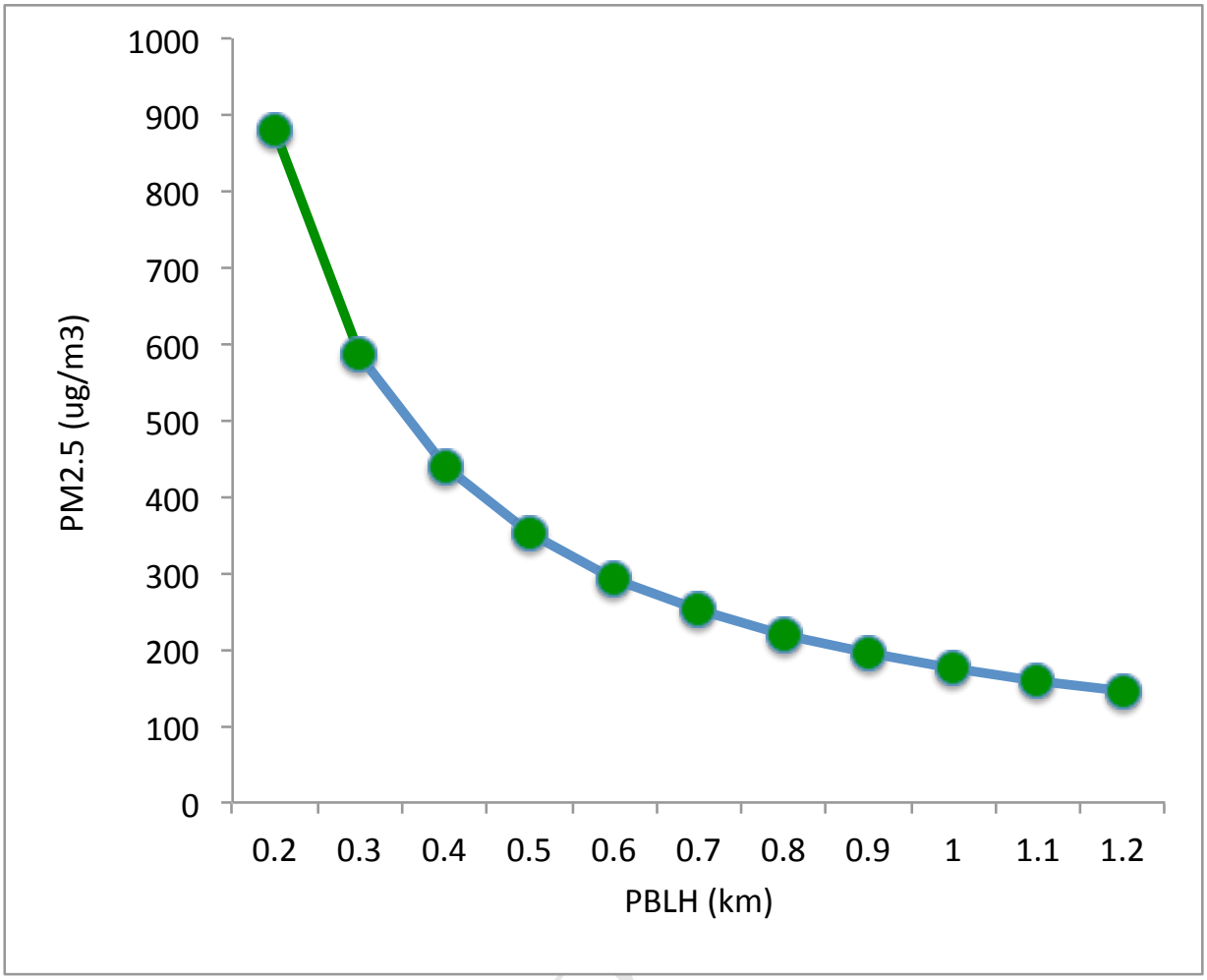

F12

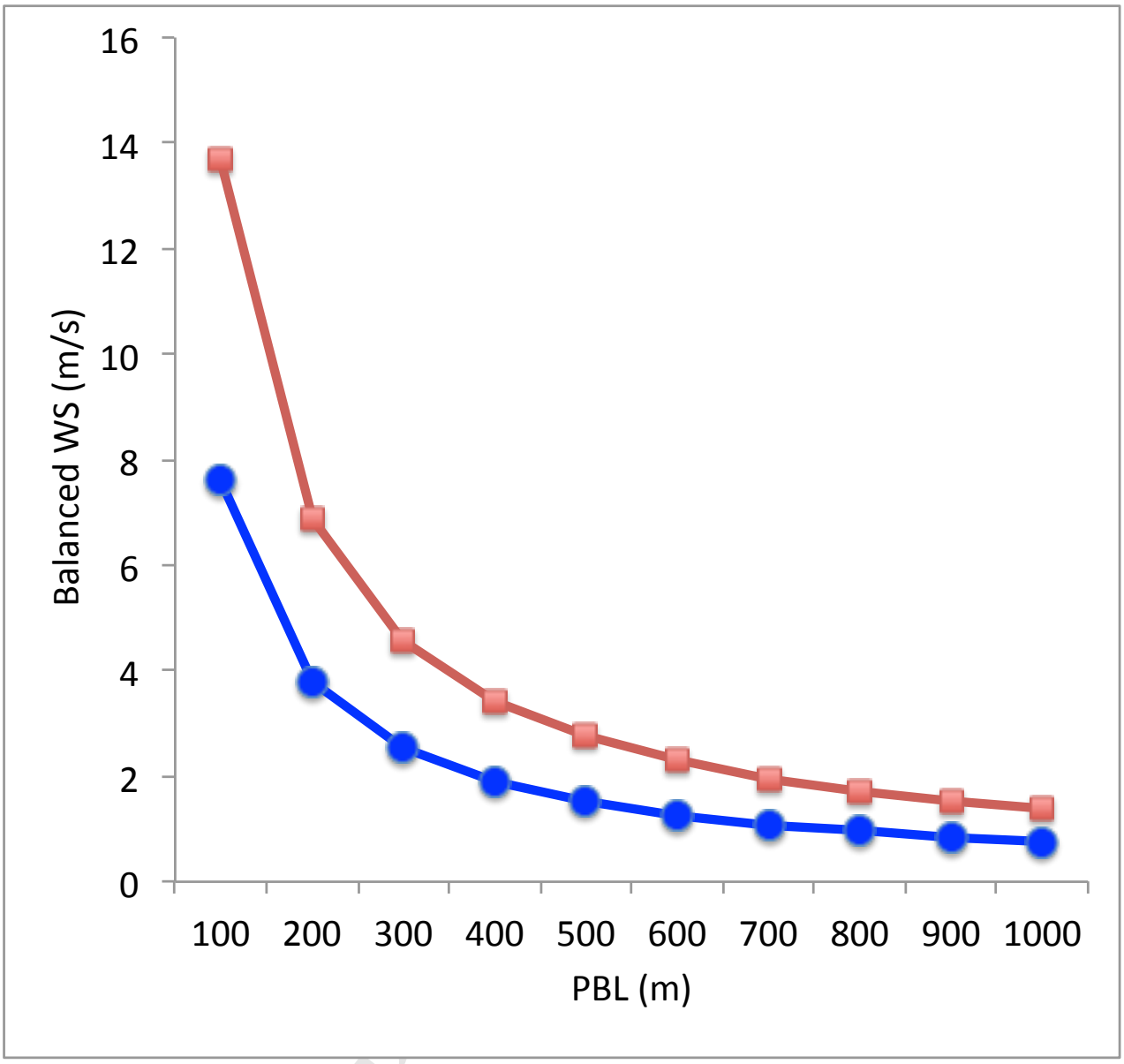
16
14
12
10
8
6
4
2
0
Balanced WS (m/s)
100
200
300
400
500
600
700
800
900
1000
PBL (m)

F13